Earthquake Engineering, Tenth World Conference © 1992 Balkema, Rotterdam. ISBN 90 5410 060 5

Interpretation of in situ dynamic soil testing

M.S. El Youssoufi, M. Mabsout & P.Jouanna
University Montpellier II & GRECO Géomatériaux, France

J.P.Touret
EDF, Centre National d'Equipement Hydraulique, Le Bourget du Lac, France

ABSTRACT: This study deals with identification of non-linear dynamic soil properties using a one-well harmonic in situ test, at high energy levels. Special casings can be expanded and can vibrate the soil vertically, a down-the-hole harmonic probe creating large cyclic displacements of the well wall at different frequencies. Accelerations behind the special casings are given by transducers placed in the soil from the surface or by down-the-hole robots. Measurement interpretation, specially studied here, requires numerical simulations of the soil behaviour. A two parameter hysteretic law is chosen here. More complicated models could be envisaged but they induce difficulties in numerical convergence and uniqueness when identifying soil parameters. These parameters are obtained by comparison of acceleration recordings and numerical accelerograms. Interpretation can be performed in the time domain and/or the frequency domain, where harmonics are generated by non-linearities of the soil.

1 INTRODUCTION TO THE ONE-WELL SV HARMONIC TECHNIQUE

1.1 Objectives of the one-well harmonic test

To measure seismic soil characteristics under the most severe earthquakes, no satisfactory in situ test is available for strains up to 10^{-3} (Haghgou 1985). The features of the one-well technique proposed here are as follows (Jouanna & Montiel 1988, EDF SEPTEN 1990):

(i) A one-hole method is preferred to cross-hole tests to concentrate energy in the vicinity of the excitation well where non-linearities occur.

(ii) The seismic source at the well is harmonic, to simplify the identification procedure. However other signals can also be imposed.

(iii) Gauges are placed inside the soil, avoiding the disturbed soil zone around the casing.

1.2 Test configuration

The first in situ tests are under development in two 200 mm diameter wells drilled into a silty soil (0-8.00m) and a detritic formation (8.00m-12.00m).

Displacements are applied to the soil via special casing sections, moved vertically and applied radially to the soil during the test by a down-the-hole excitation probe.

Vertical displacements are created at point A and accelerations are registered at points B, C, D and E (Figure 1), by means of 3-Dim accelerometers placed into the soil by surface or down-the-hole robots.

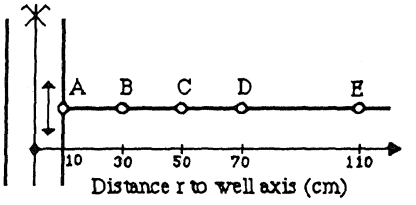

Fig.1 Test configuration

2 MODELLING OF SEISMIC SOIL BEHAVIOUR

2.1 Choices and assumptions

The soil is assumed to be homogeneous, isotropic and monophasic. In the vicinity of the well, propagation is assumed to be radial and material movement purely vertical , enabling use of 1-Dim models.

For strain less than 10^{-4}, linear visco-elastic behaviour laws can be extended to non-linear situations, semi-analytical reference solutions being available (El Youssoufi, Heitz et al. 1990, Heitz 1992).

For larger strains, cyclic hysteretic behaviour laws are adopted with Hardin and Drnevitch's first loading curve (Hardin 1972) & Masing's construction (Masing 1926).

Identification uniqueness of soil parameters is ensured with such a simple model. More sophisticated models with a larger number of parameters lead to indeterminations in the inverse problem. Moreover convergence problems which are already complex with simple models, would become intricate. The model adopted here seems to be a good compromise.

2.2 Dimensional equations

Model equations include momentum balance and relations between strains and displacements:

(1) $\tau_{,r}(r,t) + \frac{\tau(r,t)}{r} = \rho\, \ddot{w}(r,t)$

(2) $\gamma(r,t) = \frac{2(\tau(r,t)-\delta\tau_0(r))}{2G_0+\beta\alpha(\tau(r,t)-\delta\tau_0(r))} + \delta\gamma_0(r)$

If $\delta=0$ and $\beta=-2$, first loading

If $\delta=\beta=1$, τ and γ are decreasing

If $\delta=\beta=-1$, τ and γ are increasing

(3) $\gamma(r,t) = w_{,r}(r,t)$

r = horizontal distance to the axis z ; t = time

ρ = specific mass of the soil.

$\tau(r,t)$ = vertical shear stress in the soil

$\gamma(r,t)$ = vertical shear strain of the soil

$w(r,t)$ = vertical material displacement of the soil.

$\ddot{w}(r,t)$ = vertical material accceleration of the soil.

$\tau_0(r) = |\tau|_{max}$ and $\gamma_0(r) = |\gamma|_{max}$

G_0 = shear modulus at very low strain level

α = parameter characterizing non-linearities

The stress-strain relationship (2) depending on the two soil parameters Go and α also depends on coefficients δ and β which make it possible to build the first loading curve and the hysteretic loop.

Moreover a non-linear and non-dissipative model is associated to the preceding one to investigate the differences between non-linearities and dissipation effects. It is described by the same relation (2) with the following coefficients : $\delta=0$, $\beta=-2$ (for τ and $\gamma \geq 0$) and $\delta=0$, $\beta=+2$ (for τ and $\gamma \leq 0$).

2.3 Dimensionless equations

The above equations (1) to (3) can be written in a dimensionless form taking as reference r_0 (well radius), G_0 and $T_0=1/f_0$ (period of the sinusoidal excitation).

Consequently, dimensionless variables are:

$r^*=r/r_0$, $t^*=t/T_0$

and dimensionless parameters are:

$r^*_0 = 1$; $G^*_0=1$; $T^*_0=1$;

$R^*_0 = R_0/r_0$; $\rho^* = \rho / (\frac{G_0 T_0^2}{r_0^2})$; $W^*_A = W_A/r_0$

with W_A= amplitude of displacement at point A.

Unknowns are written in a dimensionless form :

$\tau^*=\tau/G_0$; $\gamma^*=\gamma$; $w^*=w/r_0$; $\ddot{w}^* = \ddot{w}/(\frac{r_0}{T_0^2})$

Forgetting all stars for reasons of simplicity, the dimensionless equations, used in the following, are :

(4) $\tau_{,r}(r,t) + \frac{\tau(r,t)}{r} = \rho\, \ddot{w}(r,t)$

(5) $\gamma(r,t) = \frac{2(\tau(r,t)-\delta\tau_0(r))}{2+\beta\alpha(\tau(r,t)-\delta\tau_0(r))} + \delta\gamma_0(r)$

If $\delta=0$ and $\beta=-2$, first loading

If $\delta=\beta=1$, τ and γ are decreasing

If $\delta=\beta=-1$, τ and γ are increasing

(6) $\gamma(r,t) = w_{,r}(r,t)$

The dimensionless form of the non-dissipative associated model is immediately deduced.

3 DIRECT PROBLEM RESOLUTION

The Finite Difference Method is well adapted to this 1-Dim numerical integration. However this method, especially in a dynamic situation, requires finding an appropriate discretization, satisfying consistency, stability and convergence criteria. These problems, related to the hysteretic model, are studied here for simplicity on the associated model, without introducing any fundamental restriction.

3.1 Discretization and algorithm of resolution

Value of γ given by equation (6) can be placed in equation (5), leading to :

(7) $\tau_{,r} + \frac{\tau}{r} = \rho \ddot{w}$

(8) $w_{,r} - \frac{\tau}{1-\alpha|\tau|} = 0$ (associated model)

Fixed space steps and a total implicit scheme are adopted for obtaining the following discretized dimensionless equations :

(9a) $\frac{\tau_{i+1,n} - \tau_{i-1,n}}{2\Delta r} + \frac{\tau_{i,n}}{R(i)} - d\,w_{i,n}$

$= d(-2\,w_{i,n-1} + w_{i,n-2})_{known}$ $\quad (2 \leq i \leq N-1)$

(9b) $(1 - \frac{1}{\Delta r})\tau_{1,n} + \frac{1}{\Delta r}\tau_{2,n}$

$= d(w_{1,n} - 2\,w_{1,n-1} + w_{1,n-2})_{given}$ $\quad (i=1)$

(9c) $-\frac{1}{\Delta r}\tau_{N-1,n} + (\frac{1}{\Delta r} + \frac{1}{R(N)})\tau_{N,n} =$

$= d(w_{N,n} - 2\,w_{N,n-1} + w_{N,n-2})_{elastic}$ $\quad (i=N)$

(10a) $\frac{\tau_{i,n}}{1-\alpha|\tau_{i,n-1}|} - \frac{w_{i+1,n} - w_{i-1,n}}{2\Delta r} = 0$ $\quad (3 \leq i \leq N-2)$

(10b) $\frac{\tau_{2,n}}{1-\alpha|\tau_{2,n-1}|} - \frac{w_{3,n}}{2\Delta r} = (-\frac{w_{1,n}}{2\Delta r})_{given}$ $\quad (i=2)$

(10c) $\frac{\tau_{N-1,n}}{1-\alpha|\tau_{N-1,n-1}|} + \frac{w_{N-2,n}}{2\Delta r} = (\frac{w_{N,n}}{2\Delta r})_{elastic}$ $\quad (i=N-1)$

i= space index(=1 well wall; =N boundary);

Δr= space step; n = time index; Δt= time step;

$d = \frac{\rho}{\Delta t^2}$; $R(i) = 1 + (i-1)\Delta r$ for $1 \leq i \leq N$,

R(i) being the dimensionless distance to the well axis.

This set of equations is linear in $\tau_{i,n}$ and $w_{i,n}$ when values at time n-1 and n-2 are assumed to be known. The difficulty due to the non-linear term occurring in the denominator of expression (8) is overcome by estimating this term at time n-1.

3.2 Consistency

The difference between the exact differential operator (7) + (8) and the approached discretized operator (9)+(10) should tend to zero, when Δr and Δt tend to zero, to insure consistency. Truncation errors ε_1 on operator (7) and ε_2 on operator (8) are given below using Taylor's developments in space (at order 1) and time (at order 2) :

$$\varepsilon_1 = + \sum_{k=2}^{\infty} \frac{(2\Delta r)^{k-1}}{k!} \frac{\partial^k \tau}{\partial r^k} - 2\rho \sum_{k=2}^{\infty} \frac{(\Delta t)^{2(k-1)}}{(2k)!} \frac{\partial^{2k} w}{\partial t^{2k}}$$

$$\varepsilon_2 = + \sum_{k=2}^{\infty} \frac{(2\Delta r)^{k-1}}{k!} \frac{\partial^k w}{\partial r^k}$$

As truncation errors ε_1 and ε_2 tend to zero when Δr and Δt tend to zero, the adopted discretization scheme insures consistency for both operators (7) and (8).

3.3 Stability

As the standard discretized equations (9a) and (10a) involve three time levels, it is convenient for the stability study to introduce a third numerical variable v; three dimensionless equations replace the two equations above:

$$(11)\ \frac{\tau_{i+1,n}-\tau_{i-1,n}}{2\Delta r} + \frac{\tau_{i,n}}{R(i)} - d w_{i,n} = d(-2w_{i,n-1} + v_{i,n-1})$$

$$(12)\ \frac{\tau_{i,n}}{1-\alpha|\tau_{i,n-1}|} - \frac{w_{i+1,n}-w_{i-1,n}}{2\Delta r} = 0$$

$$(13)\ v_{i,n} = w_{i,n-1}$$

Fourier's series developments of $\tau_{i,n}$, $w_{i,n}$ and $v_{i,n}$, in the space domain, can be written as follows for the different harmonics m, with $k = 2\pi/(R_0-1)$:

$$\tau_{i,n} = \sum_m A_m^n e^{jkmi\Delta r}$$

$$w_{i,n} = \sum_m B_m^n e^{jkmi\Delta r}$$

$$v_{i,n} = \sum_m C_m^n e^{jkmi\Delta r}$$

Substitution of these expressions in equations (11), (12) and (13) gives, for each harmonic m :

$$(14m)\ A_m^n \left(\frac{j}{\Delta r}\sin km\Delta r\right) + \frac{1}{R(i)} - dB_m^n = d(-2B_m^{n-1} + C_m^{n-1})$$

$$(15m)\ \frac{1}{1-\alpha|\tau_{i,n-1}|} A_m^n - B_m^n \left(\frac{j}{\Delta r}\sin km\Delta r\right) = 0$$

$$(16m)\ C_m^n = B_m^{n-1}$$

The term $|\tau_{i,n-1}|$ is considered as a fixed coefficient.

These equations in a matrix form lead to:
$[H_m^n]U_m^n = [H_m^{n-1}]\ U_m^{n-1}$ with :

$$(U_m^n)^T = (A_m^n, B_m^n, C_m^n)^T ; (U_m^{n-1})^T = (A_m^{n-1}, B_m^{n-1}, C_m^{n-1})^T$$

Amplification matrix $[G_m^n] = [H_m^n]^{-1}[H_m^{n-1}]$ is :

$$[G_m^n] = \frac{1}{D_m} \begin{bmatrix} 0 & 2d\left(\frac{j}{\Delta r}\sin km\Delta r\right) & -d\left(\frac{j}{\Delta r}\sin km\Delta r\right) \\ 0 & 2d\,\frac{1}{1-\alpha|\tau_{i,n-1}|} & -d\,\frac{1}{1-\alpha|\tau_{i,n-1}|} \\ 0 & D_m & 0 \end{bmatrix}$$

$$D_m = -\left(\frac{j}{\Delta r}\sin km\Delta r + \frac{1}{R(i)}\right)\frac{j}{\Delta r}\sin km\Delta r + d\,\frac{1}{1-\alpha|\tau_{i,n-1}|}$$

The stability conditions are based on the study of eigen values λ of $[G_m^n]$, given by:

$$\lambda_0 = 0;\ \lambda_1 = \frac{1}{1+\sqrt{B_m}\exp(j\beta/2)} ;\ \lambda_2 = \frac{1}{1-\sqrt{B_m}\exp(j\beta/2)}$$

with $B_m\exp(j\beta) = 1 - \frac{D_m}{a}$ and $a = d\,\frac{1}{1-\alpha|\tau_{i,n-1}|}$

A necessary and sufficient condition of stability according to Von Neumann's criterion implies that the spectral radius of $[G_m^n]$ be < 1, i.e. $|\lambda_i| < 1$, (i=0,2), except for perhaps one of these values which can be equal to 1. Thus stability requires :

$$|\lambda_1|^2 = \frac{1}{|1+\sqrt{B_m}\exp(j\beta/2)|^2} \le 1 \ ; |\lambda_2|^2 = \frac{1}{|1-\sqrt{B_m}\exp(j\beta/2)|^2} \le 1$$

This condition has to be fulfilled for any m . Unfortunately for m=0, $|\lambda_1|$ and $|\lambda_2| = 1$. In this case, the above conditions are necessary but not sufficient for stability . They can be transformed into a necessary and sufficient condition of instability written :

$$(17)\ \Delta r \ge \frac{\Delta t}{\rho^{1/2}} \frac{\pi}{N} (1 + 1/4\pi^2)^{1/4}\ |(1-\alpha|\tau_{i,n-1}|)|^{1/2}$$

3.4 Convergence

A finite difference scheme is said to be convergent if the difference between the numerical solution and the true solution tends to zero when Δr and Δt tend to zero. According to Lax's theorem, consistency and stability are equivalent to convergence if the problem is well posed(unique solution and sufficiently smooth boundary conditions) and if the problem is linear. In the case of a non-linear problem, it is assumed that this equivalence still holds, insofar as non-linearities do not generate multiple and non physical solutions.

3.5 Algorithm of resolution

In the case of the non-linear non dissipative model, the 2N-2 values of $\tau_{i,n}$ (i=1,N) and $w_{i,n}$ (i=2,N-1) at time $n\Delta t$ are obtained by solving the 2N-2 equations (9) and

(10) which are linear in $\tau_{i,n}$ and $w_{i,n}$, the values $\tau_{i,n-1}$, $w_{i,n-1}$ and $w_{i,n-2}$ being given by the preceding iteration. Computation begins at n=3; the 2 first steps are deduced from the elastic analytical solution (α=0).

In the case of the non-linear and dissipative model, first loading is identical to the above procedure up to the maximum τ_o, using values of δ=0 and β= -2 in equation (5). Next, the decreasing branch of the stress-strain cycle is described using δ=β=1 in equation (5). When the minimum value - τ_o is obtained, the increasing branch of the stress-strain cycle is given by equation (5) with δ=β=-1.

3.6 Sensitivity of stability to numerical parameters

Due to the lack of a necessary and sufficient stability criterion, tests of convergence are to be performed for each set of boundary conditions as follows:

(i) In the linear elastic case (α= 0), the numerical solution is compared to the analytical solution.

(ii) In the non-linear elastic case($\alpha \neq$ 0), the numerical solution is compared to a semi-analytical solution (Heitz 1992).

(iii) In the hysteretic case comparison can be made with the preceding semi-analytical solution. However this reference solution is based on a non-linear visco-elastic behaviour and does not take hysteretic phenomena into account ; moreover, its stability requires the condition $\alpha.\gamma_0(r) < 1$ which is a limitation for high strain values.

Ilustrations are given below for the following dimensional conditions :

r_0= 0.1m ; $\rho = 2.10^3$ kg/m^3. At the well wall (point A), excitation is purely harmonic with $W_A = 4\ 10^{-4}$m, i.e. $\gamma_{A\ max} \cong 1.0\ 10^{-3}$. At the outer boundary , $w(R_0, t)$ is assumed be equal to the linear analytical value.

(i) Linear elastic case (α= 0) :

Maximum dimensionless acceleration $\ddot{W}_{max}$ versus dimensionless distance r'* to the well wall is given in Figure 2, where a comparison is made between linear computation and analytical solution for :

R_0=0.6m (Figure 2a) and 1.1 m (Figure 2b)

$\Delta r = (R_0 - r_0)/40$ and $\Delta t = T_0/128$.

This requires the inversion of a 80x80 matrix, its rank being equal to twice the number of discretization points. Here R_0=1.1 m seems to be the maximum value consistent with good convergence. If higher values of R_0 are desired, the rank of the matrix must be increased.

(ii) Non-linear and non dissipative case ($\alpha \neq 0$) : Computation is the same except that the matrix coefficients have to be updated at each time step, here 128 times per period. Figure 3a gives in the same conditions as in (i), except that α = 2000, the acceleration variation at point B versus time and Figure 3b gives its Fourier transform, where odd harmonics only are created by non-linearities.

(iii) For the hysteretic case, the preceding computation takes into account the stress-strain cycle. An example of acceleration variation at point B, versus time, is given on Figure 4a and its Fourier transform in Figure 4b.

4 INVERSE IDENTIFICATION PROCEDURE

4.1 Proposed identification procedure

The model depends on two parameters, the first parameter G_0 being characteristic of the elastic property of the soil at low strains and the second coefficient α governing non linearity effects and dissipation (Masing's rule). It is possible to decouple the determination of these two parameters by an inverse process.

This procedure is relatively simple when the signal is purely harmonic. However it can become more complicated if the signal delivered at the well is affected by some noise, which interfere with signal modifications due to non linearities of the soil. Furthermore, some soil disturbance can result from drilling around the well.

4.2 Determination of parameter G_0

4.21 Ideal case of a pure harmonic signal w_A at the well

Experiments in the linear domain, i.e.with small displacements W_A at the well, can be interpreted to determine G_0 by different procedures:

- Phase method: the classical time arrival method can be adapted to an harmonic excitation test by studying the phase difference between acceleration signals measured at points r_1 and r_2. The propagation velocity v_s can be deduced from this phase difference, leading to the value of $G_0 = \rho\ v_s^2$.
- Amplitude method: the ratio betwen the modulus of the purely harmonic acceleration signals measured at points r_1 and r_2 can be compared to the analytical value of this ratio, leading to G_0 by :

$$\frac{|K_0(jkr_2)|}{|K_0(jkr_1)|} = \frac{|\ddot{W}_0(r_2,\omega_0)\text{measured}|}{|\ddot{W}_0(r_1,\omega_0)\text{measured}|}$$

with $k = \dfrac{\omega_0}{(G_0/\rho)^{1/2}}$ and K_0= modified Bessel function of second kind and zero order.

Different frequencies can be used to operate an averaging. The experimental points are plotted on a graph of transfer functions corresponding to different G_0 values. By matching, the best approximation leads to the value of G_0.

4.22 Case of a noisy signal w_A at the well

At low levels of excitation, if the displacement w_A is not purely harmonic due to noise, it is possible to make a Fourier transform, the phenomena being linear, and then operate as previously.

4.23 Case of a noisy signal w_A at the well and an altered soil around the well

If moreover some disturbance of the soil is assumed to take place around the well during drilling, the preceding method can be applied between two acceleration readings at points B, C, D, etc. , avoiding taking into account recordings in the disturbed zone around the well.

4.3 Determination of parameter α

4.31 Ideal case of a pure harmonic signal w_A at the well

Assuming a large but purely harmonic displacement W_A applied at the well, accelerations recorded at points B, C, D, etc. are no longer sinusoidal because they are affected by soil non-linearities. Accelerations at a given point M can be obtained if a value of α is assessed, G_0 being given as described above. Thus at each point M a set of acceleration versus time curves can be plotted depending on different possible α values, under a given displacement W_A at the well.

Comparing the registered acceleration versus time curves at point M with the set of acceleration curves deduced from computation at the same point M, leads by matching to a proposed value of parameter α. Averaging can be done at different points M. However the most significant results are obtained in the neighbourhood of the well, where non-linearities occur.

This matching can also be done, or verified, in the frequency domain, by comparing the different harmonics obtained by numerical simulation and obtained by a Fourier transform of the experimental acceleration recordings.

4.32 Case of a noisy signal w_A at the well

At high levels of excitation, if the signal w_A at the well is altered by noise, the preceding method still holds, except that w_A has to be registered. Small disturbances in the input can create high disturbances in the acceleration outputs, affected by the square of the frequency.

4.33 Case of a noisy signal w_A at the well and of an altered soil around the well

If the soil is altered around the well, the same procedure could be applied between to inner points, B and C for instance. Point B can be considered as the excitation point and C the receiver. Displacement at point B is not measured, but can be obtained by integrating twice the registered acceleration at point B. Numerical stability of this integration can be ensured by integrating twice a Fourier transform of the acceleration.The problem is identical to the preceding one, except that the noisy signal is imposed at point B instead of point A.

5 CONCLUSION

Determination of dynamic soil properties requires working in the vicinity of the energy source to obtain high strains. The one-well harmonic in situ test has been designed to fulfill such conditions. However a careful identification process has to be set up. Attention has to be paid to the choice of models; when they are too simple they ignore hysteretic effects and when too complex they lead to non convergence or non uniqueness situations.

Hysteretic models, as used here, prohibit the use of analytical or semi-analytical approaches for obtaining numerical accelerograms. Numerical finite difference procedures, in such highly dynamic phenomena, encounter convergence difficulties, even in the simplest case of 1-Dim and pure shear models. If consistency is satisfied here, a necessary and sufficient stability condition is not available; this fact leads to a careful procedure for checking the reliability of the numerical results, by a series of comparisons with analytical or semi-analytical methods when possible.

Identification problem can be solved in the time domain or in the frequency domain, using harmonics due to non-linear and hysteretic effects. The problem is simple with a pure harmonic displacement source at the well. However, in practice the process is more complicated due to the sensitivity of acceleration to noise. Moreover, disturbance of the soil around the well implies using only internal soil measurements and a more sophisticated interpretation process.

Finally, the precision obtained on soil parameters relies first on the quality of the experimental device, which should ensure an input signal as pure as possible, disturbance of the soil around the well as small as possible and excellent transmission of the recorded acceleration signals. On the other hand, quality of the behaviour model and numerical procedure are essential for comparing recordings and numerical accelerograms.

REFERENCES

EDF SEPTEN 1990. Projet d'instrumentation in situ monopuits pour la reconnaissance de caractéristiques sismiques de sols. *Contrat ND 1000.* EDF/SEPTEN-CNRS 13°Circonscription. France.

El Youssoufi, M.S., Heitz, J.F., Bonnet, G., Jouanna, P., 1990. Principes d'identification de caractéristiques dynamiques non-linéaires de sols, en essais harmoniques in situ monopuits. *Journées d'Etudes "Diagraphies et mécanique des terrains".* 13 et 14 novembre. Bordeaux. France.

Haghgou, M. 1985. Mesure in situ de l'amortissement interne des sols. Etude bibliographique. Gières: Sol Engineering. France.

Hardin, B.O., Drnevich, V.P. 1972. Shear Modulus and Damping in Soils: Design Equations and Curves. *Journal of the Soil Mechanics and Foundations Division. Proceedings of the ASCE.* Vol. 98. No. SM7. July. 667-692.

Heitz, J.F 1992(to be published). Propagation d'ondes en milieu non-linéaire. Applications au génie parasismique et à la reconnaissance des sols. *Thèse de Doctorat..* Univ. Joseph Fourier. Grenoble. France.

Jouanna, P. & Montiel, A. 1988. Elément de cuvelage et dispositifs d'excitation pour la détermination des caractéristiques dynamiques du terrain dans un forage. *Brevet N°88 09254.* 7juillet 1988. Paris. France.

Masing G. 1926. Eigenspannungen und Verfestigung beim Messing. *Proc. 2nd International Congress of Applied Mechanics.* Zurich. Switzerland.pp. 332-335.

ACKNOWLEDGMENTS

The authors are grateful to ELECTRICITE DE FRANCE for the help given by the contract ND1000 CNRS Montpellier -EDF SEPTEN Lyon and to the CNRS for the help given by GRECO Géomatériaux.

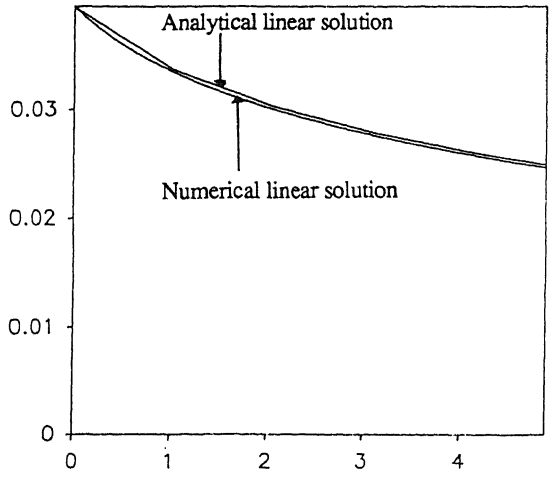

Fig.2a Variations of $\ddot{W}^*_{max}$ versus r'* (R_o = 0.6 m)

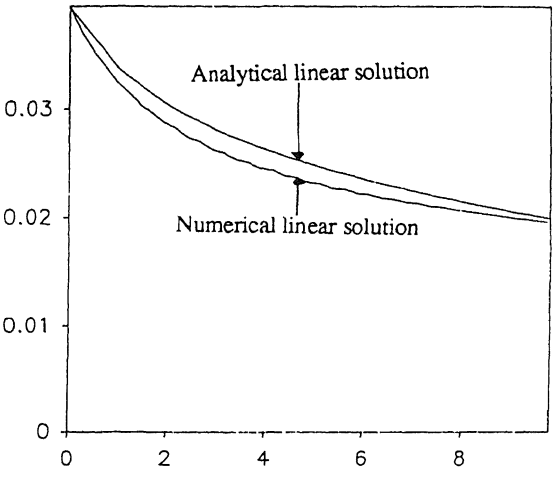

Fig.2b Variations of $\ddot{W}^*_{max}$ versus r'* (R_o = 1.1 m)

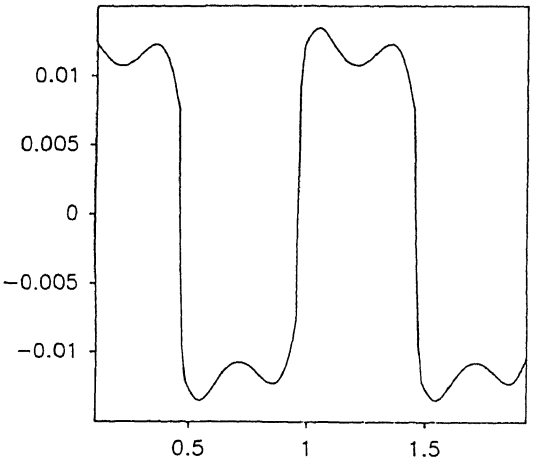

Fig.3a $\ddot{w}^*(R_B,t^*)$. Non-linear case

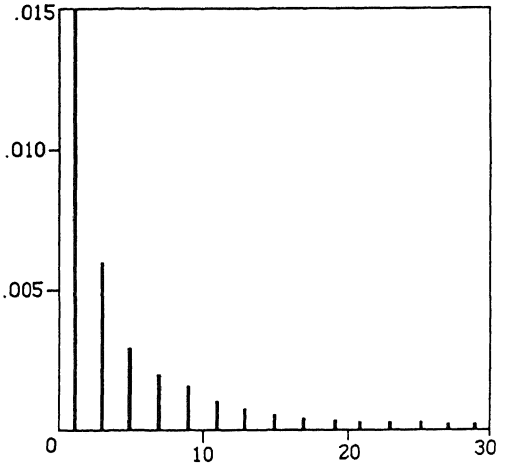

Fig.3b $|\ddot{w}^*(R_B,f^*)|$. Non-linear case

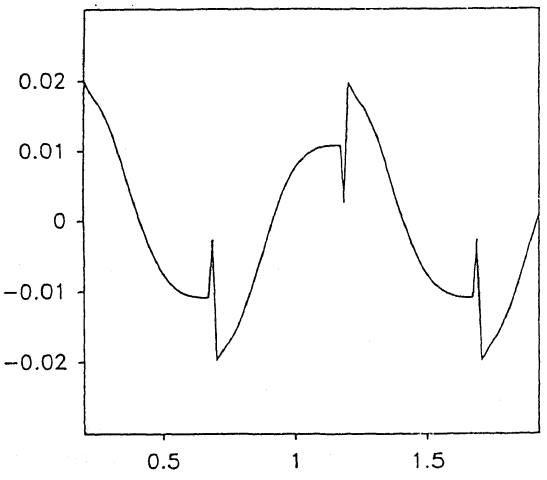

Fig.4a $\ddot{w}^*(R_B,t^*)$. Hysteretic case

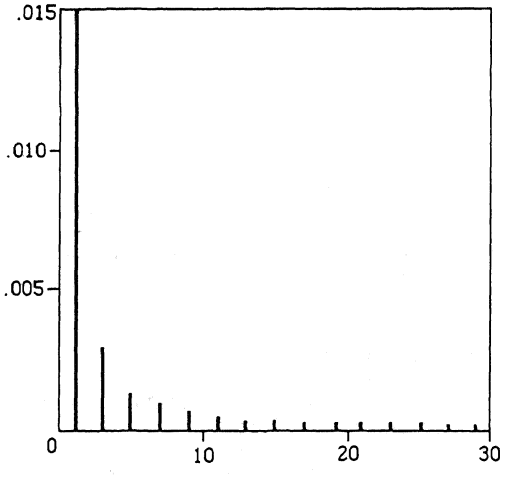

Fig.4b $|\ddot{w}^*(R_B,f^*)|$. Hysteretic case